

RESEARCH ARTICLE

Video Detection of Small Leaks in Buried Gas Pipelines

YUXIN ZHAO¹, ZHONG SU¹, (Member, IEEE), HAO ZHOU, AND JIAZHEN LINSchool of Automation, Beijing Information Science and Technology University, Beijing 100192, China
Beijing Key Laboratory of High Dynamic Navigation Technology, Beijing 100192, China

Corresponding author: Zhong Su (sz@bistu.edu.cn)

This work was supported in part by the National Key Research and Development Program of China under Grant 2020YFC1511702 and Grant 2022YFF0607400; in part by the National Natural Science Foundation of China under Grant 61971048; in part by the Beijing Science and Technology Project under Grant Z221100005222024; and in part by the Beijing Scholars Program, Key Laboratory of Modern Measurement and Control Technology, Ministry of Education.

ABSTRACT For the problem of difficult tracking of small leaks in buried gas pipelines, a video detection of small leaks in buried gas pipelines method is proposed for the detection robot inside buried gas pipelines. Firstly, collecting images and videos of leaks inside buried gas pipelines to establish a dataset. Secondly, build a video detection model for small leaks in buried gas pipelines, introduce a bidirectional feature pyramid network into YOLOv5s (You Only Look Once), and build a feature fusion network to enhance the model's ability to fuse small leaks. Thirdly, building a small target detection layer and a small target detection head in the YOLOv5s classification prediction network enhances the model's ability to fuse small leaks. Fourthly, the video detection model for small leaks in buried gas pipelines is trained using the dataset. Lastly, the model's video detection effect of small leaks is verified through leak detection experiments in various situations. The experimental results show that the precision rate of this method is 94.1%, the recall is 94.8%, and the average precision is 94.5%, which has a good detection effect and strong generalization ability.

INDEX TERMS Video detection method, small leaks, buried gas pipelines.

I. INTRODUCTION

Gas pipeline is widely used in gas transportation because of its advantages of continuous transmission, large transmission capacity, convenience, high efficiency, and so on, which brings a lot of convenience and economic benefits for daily life and industrial production [1]. Gas pipeline volume is large, wide area, to reduce the area, the vast majority of gas pipelines are buried in the ground, with the burial time getting longer and longer, the gas pipeline will inevitably appear problems [2]. Holes, cracks, etc. will lead to pipeline leakage, gas pipeline leakage will not only cause energy waste, economic loss, and serious explosion, threatening the safety of people's lives and property, so regular overhaul of the gas pipeline is necessary [3], [4].

The current gas pipeline detection methods include acoustic emission signal detection [5], negative pressure wave

detection [6], wavelet detection [7], image recognition methods [8], and other methods. However, the acoustic emission signal detection method, negative pressure wave detection method, and wavelet detection method can only detect large leaks, and can't detect the leakage of early holes, cracks, and other early small leakage characteristics, the picture recognition method can identify small leaks, but the method can only leakage identification of a single image, can't be continuous tracking of the leakage, easy to have been detected leakage is mistaken for a new leakage problem, for the subsequent It is easy to mistake the detected leaks for new leaks, which brings uncertainties for the subsequent troubleshooting.

To solve the above problems, this paper proposes a video detection method for small leaks in buried gas pipelines and builds a video detection model for small leaks in buried gas pipelines. Taking the pipeline inspection robot as the shooting carrier, collecting images and videos of buried gas pipeline leakage expanding the images, establishing the dataset, and making the corresponding labels. Improving the

The associate editor coordinating the review of this manuscript and approving it for publication was Gianluigi Ciocca¹.

feature fusion network (Neck) structure of the YOLOv5s algorithm [9], and introducing the bidirectional feature pyramid network (BiFPN) [10] into the Neck of the model, to enhance the fusion ability of the model's tiny leakage feature information, and improve the model's leakage detection precision in the YOLOv5s algorithm. Construct a small target detection layer in the classification prediction network (Head) of the YOLOv5s algorithm [11], build a tiny target detection head, enhance the tiny leakage detection ability of the model, and improve the tiny leakage recall of the model. Feed the dataset into the constructed model to train the network and learn the parameters of the model and feed the captured video into the completed trained model, verify the video detection effect of the model, and complete the video detection of small leaks in buried gas pipelines. The video detection method of small leaks in buried gas pipelines proposed in this paper can solve the pain point that image recognition methods can't realize tracking, frame the location of small leaks in the video, and continuously track the small leaks.

II. CONSTRUCTION OF VIDEO DETECTION MODEL FOR SMALL LEAKS IN BURIED GAS PIPELINES

A. YOLOV5S ALGORITHM STRUCTURE

YOLOv5s algorithm consists of three networks: feature extraction network (Backbone), feature fusion network, and classification prediction network [12], [13], [14]. Among them, Backbone extracts tiny leakage features from the video in the input model to form a feature map. The feature map output from Backbone is sent to the Neck layer for feature fusion, which fuses the tiny leakage feature information at different scales. The fused feature map output from the Neck layer is sent to the Head to predict the tiny leakage in the video, to frame, give confidence level, and continuously track the tiny leaks to realize the video detection of tiny leaks. The structure of the YOLOv5s algorithm is shown in Fig. 1.

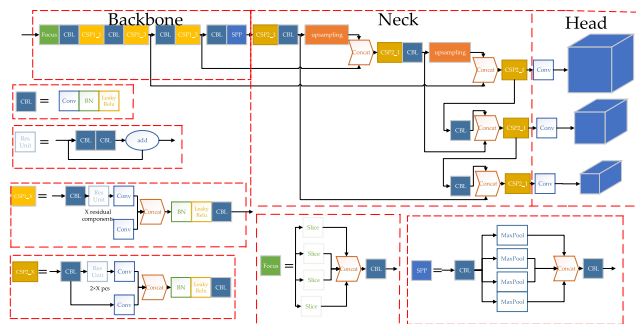


FIGURE 1. YOLOv5s algorithm structure.

B. CONSTRUCTION OF A FEATURE FUSION NETWORK

To improve the tiny leakage feature fusion capability of the model, this paper introduces the BiFPN structure into the Neck layer in the YOLOv5s algorithm, instead of the feature pyramid network (FPN) [15] + Path Aggregation

Network (PAN) [16] structure in the original structure, and the FPN+PAN structure is shown in Fig. 2.

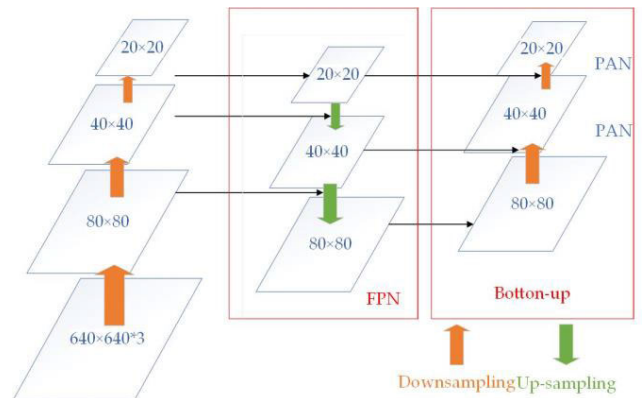


FIGURE 2. FPN+PAN structure.

The FPN+PAN structure uses a combination of up-sampling and down-sampling to realize the fusion of adjacent scale feature information, while the BiFPN structure uses a cross-scale connecting line to realize the fusion of adjacent scale and cross-scale tiny leakage feature information, which enhances the tiny leakage feature fusion capability of the model and can improve the precision of the model's tiny leakage detection. The BiFPN structure is shown in Fig. 3.

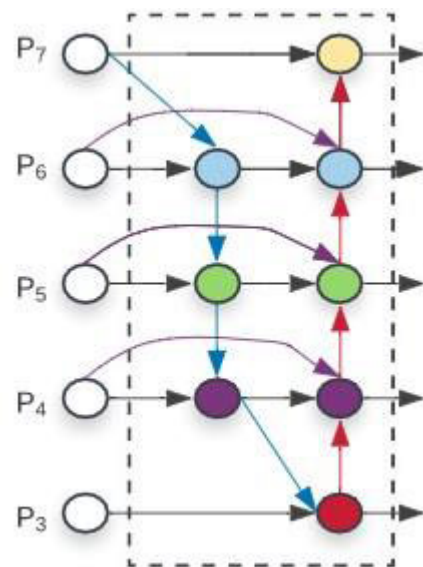


FIGURE 3. BiFPN structure.

Firstly, Backbone outputs different scales of tiny leakage feature maps into the BiFPN structure. Secondly, the BiFPN structure realizes the fusion of the first tiny leakage feature information through a transverse connection with a down-sampling operation. Thirdly, BiFPN jumps the connection through the cross-scale connecting line, realizing the fusion of the second tiny leakage feature information with the down-sampling layer and the up-sampling layer of the same scale.

Lastly, it outputs the fusion feature maps of the tiny leakage of the combination of the neighboring scales with the cross-scales to realize the fusion of the information of the tiny leakage features of the different scales.

C. CONSTRUCTION OF A CLASSIFICATION PREDICTION NETWORK

Since the leaks in buried gas pipelines in this paper are of different sizes, the smallest leak size reaches a hole-like tiny leak with a diameter of 1mm, and YOLOv5s is not ideal for the detection of such tiny targets, therefore, this paper constructs a small target detection layer in the Head layer of YOLOv5s for the detection of tiny leaks with smaller sizes. The small leakage detection head Head 1 (160×160) is newly constructed, where 160 × 160 is the feature map size, the larger the size the less feature information is contained in the feature map, so it is used for the detection of small targets, and Head 1 together with the other three detection heads in the Head layer, Head 2 (80×80), Head 3 (40×40), and Head 4 (20 × 20), form a new Head layer. Among them, Head 1 detects small leaks, Head 2 detects small leaks, Head 3 detects medium leaks, and Head 4 detects large leaks. The structure of the newly constructed Head layer is shown in Fig. 4.

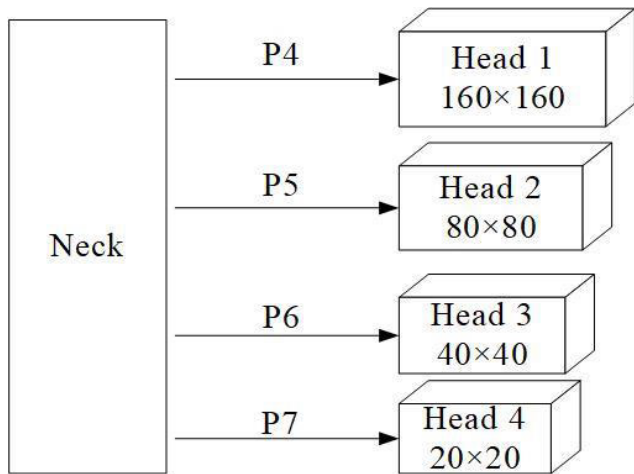


FIGURE 4. Built head layer.

The four tiny leakage feature maps P4, P5, P6, and P7 output after Neck layer feature fusion are input into four different sizes of detection heads, such as Head 1, Head 2, Head 3, and Head 4, respectively, for tiny leakage, small leakage, medium leakage, and large leakage, and then the location of the tiny leakage is boxed out in the video to show the confidence that it belongs to the leakage, and the tiny leakage is continuously tracked.

D. OVERALL CONSTRUCTION OF THE MODEL

In this paper, the original structure of the YOLOv5s algorithm, the CSPDarknet network, is used in Backbone to extract features from the video input to the model. BiFPN structure is used in the Neck layer instead of the FPN+PAN

structure of the YOLOv5s algorithm to realize cross-scale jump fusion of tiny leakage feature information and enhance the leakage detection capability of the model. Instead of the YOLOv5s algorithm, the FPN+PAN structure is used to realize cross-scale jump fusion of small leakage feature information, which enhances the leakage detection capability of the model. A small target detection layer is constructed in Head layer, and a new small leakage detection head Head 1 is built to detect small leakage, which enhances the small leakage detection capability of the model and improves small leakage recall. The structure of the buried gas pipeline small leak video detection model constructed in this paper is shown in Figure 5.

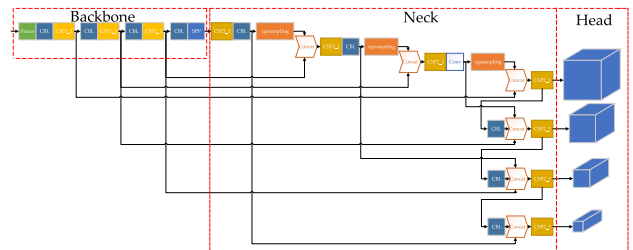


FIGURE 5. Model structure of video detection of small leaks in buried gas pipelines.

III. ESTABLISHMENT OF DATASET

A. DATASET COLLECTION PROGRAM

In this paper, the experiments used in the pipeline specifications for the outer diameter of 100mm DN100 pipe, the inner diameter of 95mm, the pipe material for the polyethylene (PE), the size of the smallest micro-leakage for the hole-like structure, the leakage size up to the diameter of 1mm. DN100 buried gas pipeline as shown in Fig. 6, which Fig. 6 (a) for the external image of the pipeline, Fig. 6 (b) for the internal image of the pipeline.

This paper proposes a buried gas pipeline small leak video detection method for pipeline detection, detection carrier for buried gas pipeline detection robot, image acquisition based on buried gas pipeline detection robot head camera, buried gas pipeline detection robot shown in Figure 7, the camera, model DVR DVR-304H, has a resolution of 7 megapixels, a CMOS sensor, a 4x optical zoom, a lens diameter of 6mm, and an image sensor size of 1/4. The buried gas pipeline inspection robot for the snake structure, through the body of 1.7m, composed of multiple sections of the function of the warehouse, contains positioning modules, corrosion detection modules, and power supply compartments, every two sections are connected by the chain, can be bent to a certain angle, used to turn in the buried gas pipeline, through the elbow, tee and other pipeline conditions. Buried gas pipeline inspection robot body around the pulley structure, the pulley structure has elasticity, used to support itself in the pipeline to fit the inner wall of the pipeline, to reduce its own rolling movement, easy to pass through the two sections of the pipeline connected to the pipeline joints.



(a) pipeline exterior image



(b) images of the inside of the pipe

FIGURE 6. DN100 buried gas pipe.



FIGURE 7. Robot for inspection in buried gas pipelines.

The head and tail of the buried gas pipeline internal inspection robot are each equipped with a camera for collecting images and video datasets, and the camera of the buried gas pipeline internal inspection robot is shown in Figure 8.

Since the buried gas pipeline is buried deep in the ground, and the in-pipe inspection robot can't hold too many devices due to its small size, the method proposed in this paper is based on the video captured and saved by the in-pipe inspection robot for detection. The head camera of the in-pipe inspection robot shoots images of the internal pathway of the

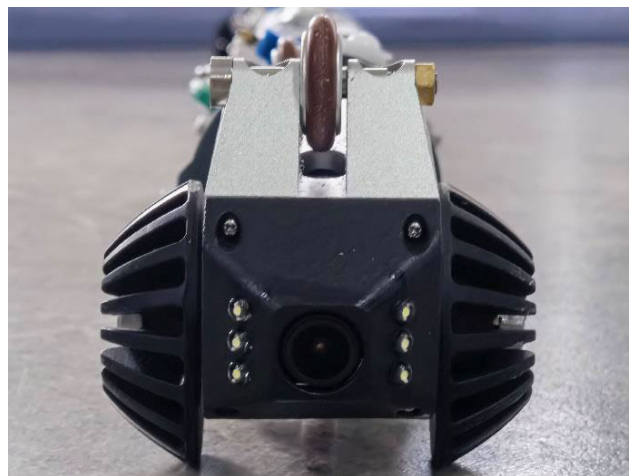


FIGURE 8. Robotic camera for inspection inside buried gas pipes.

pipeline while it is working, which is used to collect datasets and save them to the data logger, and then after the work of the in-pipe inspection robot is finished, the video detection method proposed in this paper is used to detect the small leaks in the video, and to investigate the characteristics of the early leaks in the inner wall of the pipeline. The schematic diagram of the buried gas pipeline inspection robot working in the pipeline is shown in Figure 9.

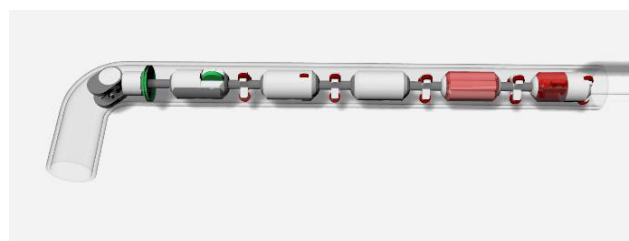


FIGURE 9. Schematic diagram of the work of inspection robot in buried gas pipeline.

B. DATASET EXPANSION

The problem of a small number of datasets is common in deep learning-based machine vision due to environmental conditions and other reasons. When the model is trained using a small number of datasets, the model suffers from overfitting, which results in the model detecting only the leaks in the dataset, and the detection of the same leaks in different scenes is very poor, so the expansion of the dataset is necessary to improve the model's generalization ability.

Augmentation of the dataset can achieve the expansion of the number of datasets, such as brightness transformation, contrast transformation, color transformation, sharpness, and other transformations, as well as rotation, shear, flip, and other image transformations [13], [14]. Based on a total of 198 datasets collected by the buried gas pipeline inspection robot, these datasets are screened, and the remaining datasets are 171 datasets after the removal

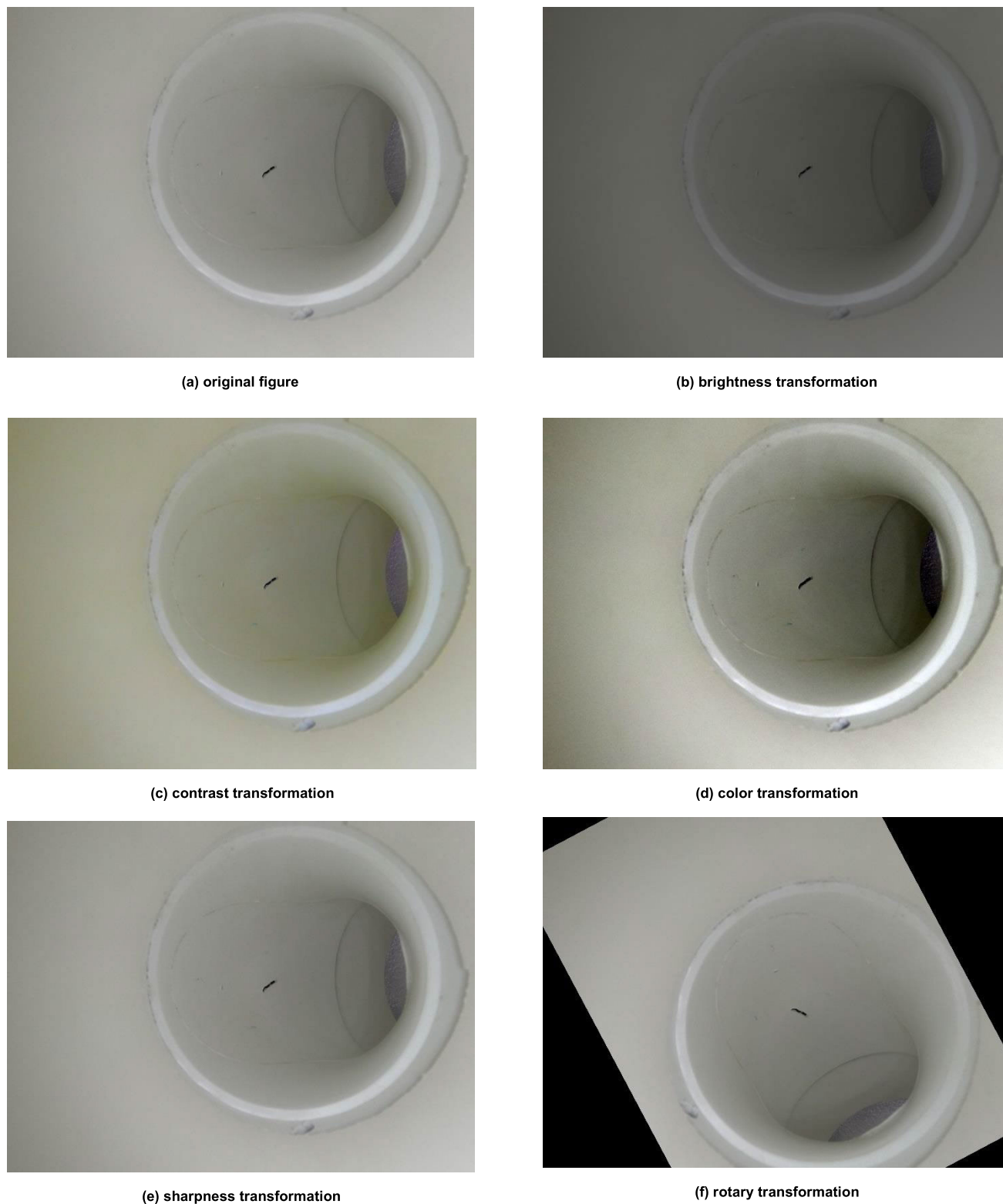


FIGURE 10. Comparison of DN100 buried gas pipeline dataset before and after expansion.

of poor-quality datasets, these 171 datasets are expanded using the above dataset expansion methods and combinations of methods, and the total number of datasets is

3,000 datasets after expansion. The comparison of datasets before and after the expansion of the dataset of the DN100 buried gas pipeline is shown in Figure 10, where



(g) shear transformation



(h) flip-flop transformation



(i) combinatorial transformation

FIGURE 10. (Continued.) Comparison of DN100 buried gas pipeline dataset before and after expansion.

Figure 10 (a), (b), (c), (d), (e), (f), (g), (h), (i) are the original image, brightness transformation, contrast transformation, color transformation, sharpness transformation, rotation transformation, shear transformation, flip transformation, and the combination of the above transformations transformed datasets.

C. CREATION OF DATASET

The expanded dataset is normalized to 640×640 size, and the 1500 datasets are annotated using the annotation tool to produce labels. On each dataset in turn, use a rectangular box to select the location of small leaks in the dataset, and name the small leaks selected by the box, because this paper only has a

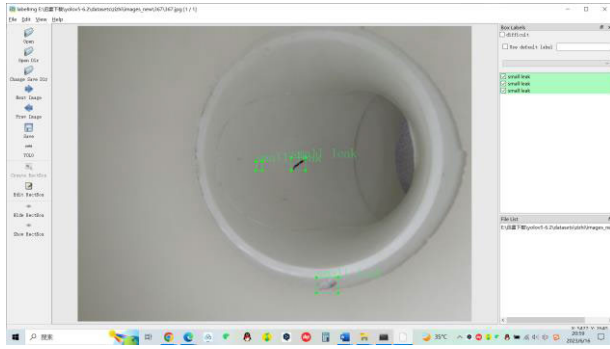
class of small leaks as a target, the naming is only small leaks a kind of. The above operations are performed sequentially on each dataset to complete the production of the corresponding label for each dataset, and the establishment of the dataset is completed, which is used for parameter learning and network training of the model. The dataset labeling results are shown in Fig. 11.

IV. RESULTS

A. EXPERIMENTAL CONDITION

1) EXPERIMENTAL ENVIRONMENT

The equipment used for the experiments in this paper is a PC with Windows 10 operating system, the central processing



(a) annotation interface

0 0.286073 0.780864 0.0208333 0.0174897 0.311928
 0 0.262635 0.904064 0.023341 0.0277778 0.758966
 0 0.310282 0.496914 0.0102238 0.0138889 0.772162

(b) label

FIGURE 11. Dataset annotation results.

TABLE 1. Experimental environment.

Serial number	Name	Configure ^a
1	operating system	Windows 10
2	CPU	Inter Core i5-13600
3	GPU	NVIDIA RTX 3060
4	RAM	16G
5	display memory	8G
6	programming software	Pycharm2022.2.3
7	deep learning framework	Pytorch1.13.0
8	programming language	Python3.8

unit (CPU) is Inter Core i5-13600, the image processor (GPU) is NVIDIA RTX 3060, the RAM is 16G, the video memory is 8G, the programming software used is Pycharm2022.2.3, the deep learning framework is Pytorch1.13.0, and the programming language is Python3.8. The experimental environment is shown in Table 1.

2) MODEL TRAINING PARAMETERS

YOLOv5s algorithm parameters initial weights using random initial weights, training rounds 300 times, using warm-up training mode, that is, in the initial rounds using a lower learning rate, to avoid large changes in the network parameters lead to model instability, the size of the image on the input side of the size of the image is 640 × 640 × 3, the training batch is 16, and the number of threads is set to 8 threads working mode. That is, 16 images are fed into the model as a batch for training, the optimizer selects stochastic gradient descent (SGD), and the number of threads is set to 8 threads working mode. The network parameters are set as shown in Table 2.

3) EVALUATION INDICATORS

Since the detection target in this paper is only one category of tiny leakage, the mean average precision (mAP), which

TABLE 2. Training parameter.

Serial number	Name	Configure ^a
1	initial weight	randomization
2	epoch	300
3	input image size	640×640×3
4	batch size	16
5	optimizer	SGD
6	works	8
7	initial learning rate	0.070492
8	Final Learning rate	0.000166

measures the comprehensive evaluation index of multi-category targets, is equal to the average precision (AP), which measures the comprehensive evaluation index of single-category targets, so in this paper, we choose the average precision, precision(P), and recall(R), i.e., the recall, as the measures of tiny leakage video detection capability of this experimental model [17]. The mathematical formulas of P, R, and AP are shown in equation (1), equation (2), and equation (3), respectively. leakage video detection capability. The mathematical formulas of P, R, and AP are shown in Eq. (1), Eq. (2), and Eq. (3), respectively.

$$P = \frac{TP}{TP + FP} \tag{1}$$

$$R = \frac{TP}{TP + FN} \tag{2}$$

$$AP = \int_0^1 P(r)dr \tag{3}$$

where TP is the number of correctly identified tiny leaks, FP is the number of false detections of tiny leaks, FN is the number of missed detections of tiny leaks, r is an integral variable, which is the integral of the product of precision and recall, and P(r) denotes the P-R curve.

B. COMPARATIVE EXPERIMENT AND ANALYSIS

To compare the YOLOv5s algorithm with the buried gas pipeline small leak video detection method proposed in this paper, this experiment sends the buried gas pipeline small leak video collected by the detection robot in the buried gas pipeline into the two models and tests the small leak video detection effect of the two models. For the same frame in the video image YOLOv5s model and the proposed buried gas pipeline small leak video detection model detection results are shown in Figure 12.

In Fig. 12, Figs. 12(a) and 12(b) are the video detection results of the YOLOv5s model and the proposed buried gas pipeline tiny leakage video detection model for the same frame of image 1 in the video, respectively. Figs. 12(c) and 12(d) are the video detection results of the YOLOv5s model and the proposed buried gas pipeline tiny leakage video detection model for the same frame of Image 2 for video detection results. Among them, the leak in Image 1



(a) YOLOv5s test results 1



(b) the results of the methodology in this paper 1



(c) YOLOv5s test results 2



(d) the results of the methodology in this paper 2

FIGURE 12. YOLOv5s and the results of the method in this paper.

and Image 2 is the same leak, and the two images are intercepted according to the chronological order of the video detection process, with a time difference of 2s.

In Image 2, there is a total of one tiny leak, located on the right inner wall of the pipe in the image, and in Image 1,

there is a total of one tiny leak, located on the right inner wall of the pipe in the image, and it can be observed from Fig. 12(a) that the YOLOv5s model can detect the point belonging to the tiny leak, but the confidence level of the point is only 30%.while in Fig. 12(b), it can be seen that



FIGURE 13. Tracking detection image.

the model proposed in this paper is also can detect the tiny leakage, but the confidence level of detecting the point is as high as 90%, which is 60 percentage points higher than that of the YOLOv5s model. From Fig. 12(c), it can be observed that the YOLOv5s model doesn't detect the tiny leakage and misses the detection, while in Fig. 12(d), it can be seen that the proposed model can detect the tiny leakage with a confidence level of 91%.

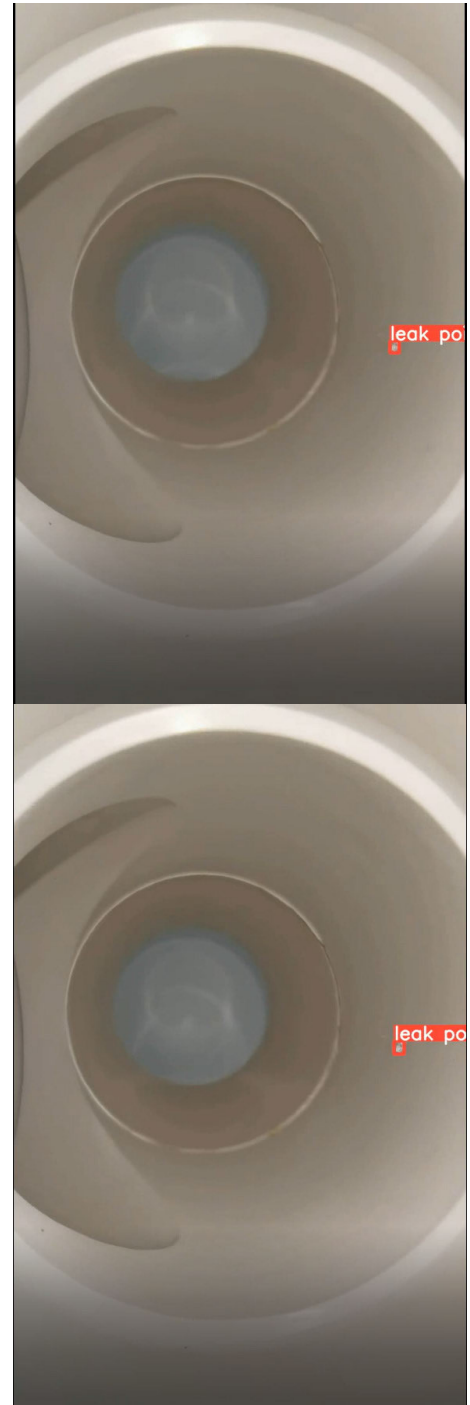


FIGURE 13. (Continued.) Tracking detection image.

From the video detection results of the above two models, it can be seen that when the YOLOv5s model can detect small leaks, this paper is also able to detect small leaks, and the confidence level is higher than that of the YOLOv5s model. When leakage detection occurs in the YOLOv5s model, the model in this paper can detect small leaks. Thus, it can be seen that the video detection method for tiny leaks in buried gas pipelines proposed in this paper is better than the YOLOv5s



FIGURE 13. (Continued.) Tracking detection image.

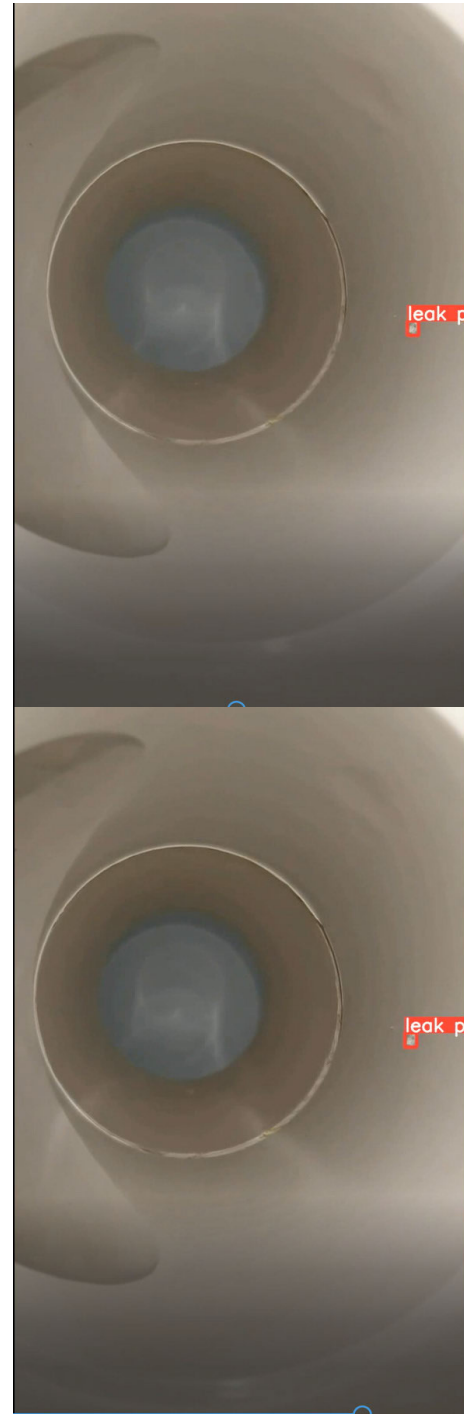


FIGURE 13. (Continued.) Tracking detection image.

model, and has a strong video detection capability for tiny leaks.

To verify the tiny leak tracking capability of the present model, the consecutive frames of the present method for tiny leak video detection are intercepted to prove that the present method can track the tiny leaks in the video continuously. The tracking detection graph is shown in Fig. 13.

To compare the video detection of tiny leaks in buried gas pipelines proposed in this paper with the tiny leak detection capability of mainstream target detection algorithms, a total of five sets of experiments were set up for the one-stage target detection algorithm SSD [18], YOLOv3 [19], YOLOv5s, CenterNet, YOLOv7, and the two-stage target detection algorithm Faster CNN [20] and other models for the tiny leak detection of buried gas pipelines, comparing the

evaluation indexes of each algorithm to evaluate the video detection effect of each model. leakage for video detection, compare the evaluation index of each algorithm to evaluate the video detection effect of each model. The results of the comparison experiments are shown in Table 3.

TABLE 3. Comparison of experimental results.

Network model	Precision/%	Recall/% a	AP/%
SSD	87.3	84.6	85.9
YOLOv3	86.1	84.0	85.1
YOLOv5	88.4	86.8	87.5
CenterNet	89.5	88.1	88.8
Faster RCNN	90.5	91.8	91.1
YOLOv7	92.0	92.9	92.5
The algorithms in this paper	94.1	94.8	94.5

As can be seen from Table 3, the YOLOv3 algorithm has the lowest evaluation index of detection results among all algorithms, with 86.1%, 84.0%, and 85.1% precision, recall, and AP, respectively. The same one-stage target detection algorithm SSD is 1.2 percentage points, 0.6 percentage points, and 0.8 percentage points higher than YOLOv3 in terms of precision, recall, and AP, respectively, and YOLOv5s algorithm precision, detection rate, and average precision are 1.1 percentage points, 2.2 percentage points, and 1.6 percentage points higher than those of SSD, reaching 88.4%, 86.8%, and 87.5%, respectively, and CenterNet's precision, detection rate, and average precision are 1.1 percentage points, 1.3 percentage points, and 1.3 percentage points higher than YOLOv5's, respectively. 89.5%, 88.1%, and 88.8%, respectively. The two-stage target detection algorithm Faster CNN is higher than all single-stage target detection algorithms except YOLOv7, with the accuracy, detection rate, and average precision reaching 90.5%, 91.8%, and 91.1%, respectively. YOLOv7, as the latest algorithm in the field of target detection, is higher than all the above algorithms in the evaluation indexes of precision rate, detection rate, and average precision, reaching 92.0%, 92.9%, and 92.5%, respectively. The three evaluation indexes of this paper's algorithm are the highest among all algorithms, which verifies that this paper's algorithm is better than the mainstream algorithms for target detection and has high evaluation indexes.

C. ABLATION EXPERIMENTS AND ANALYSIS

To verify that the detection effect of the proposed video detection method for tiny leaks in buried gas pipelines is improved due to the improvements made in this paper, i.e., the introduction of the BiFPN structure in the Neck layer of YOLOv5s and the construction of a small target detection layer in the Head layer, this paper sets up ablation experiments for YOLOv5s, YOLOv5s with the introduction of the BiFPN structure, YOLOv5s (YOLOv5s + BiFPN), YOLOv5s for constructing small target detection layer (YOLOv5s+Small Target Detection Layer), and the video detection method for tiny leakage of the buried gas pipeline proposed in this

paper (the method in this paper). The results of the ablation experiment evaluation indexes are shown in Table 4.

TABLE 4. Results of ablation experiments.

Network model	Precision/%	Recall/% a	AP/%
YOLOv5	88.4	86.8	87.5
YOLOv5s+BiFPN	91.1	89.3	90.1
YOLOv5s+small target detection layer	90.8	92.4	91.7
The algorithms in this paper	94.1	94.8	94.5

As can be seen from Table 4, the YOLOv5s model with the introduction of BiFPN structure is 2.7 percentage points higher than the original YOLOv5s model in three evaluation indexes such as precision, recall and average precision, 2.7 percentage points higher, 2.5 percentage points higher and 2.6 percentage points higher, respectively. After constructing the small target detection layer, the YOLOv5s network model is 2.4 percentage points higher, 5.6 percentage points higher, and 4.2 percentage points higher in three evaluation indexes compared to the YOLOv5s model; precision is 0.3 percentage points lower than the YOLO+ BiFPN model but higher than the YOLO5s model. Indicators are 2.4 percentage points, 5.6 percentage points, and 4.2 percentage points higher, respectively, and the precision is 0.3 percentage points lower than that of the YOLO+ BiFPN model, but the recall is 3.1 percentage points higher, and the average precision is 1.6 percentage points higher, which is because the BiFPN structure enhances the feature fusion capability of the model, which can increase the model's detection precision, and the small target detection layer is capable of detect small leaks and improve the recall of small targets. The method in this paper combines BiFPN structure and a small target detection layer at the same time, and the three evaluation indexes are the highest among all the models, reaching 94.1%, 94.8%, and 94.5%, respectively, which proves that the detection effect of the proposed method for detecting small leaks in buried gas pipelines is improved due to the improvements made in this paper.

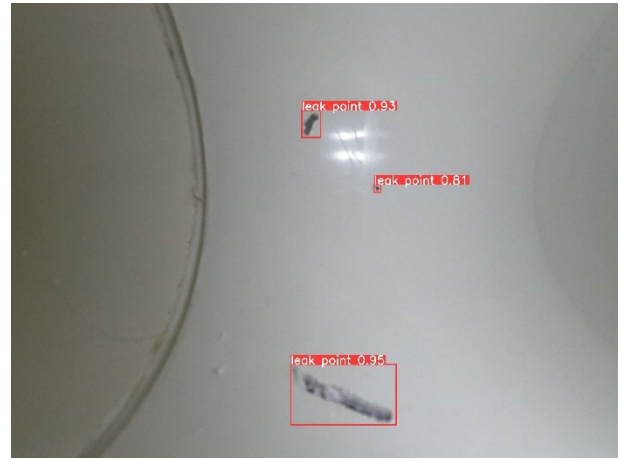
D. MULTICASE LEAKAGE EXPERIMENTS AND ANALYSIS

In this paper, for the video detection of leaks, we also conducted experiments on different shapes of leaks, different sizes of leaks, and different pipeline paths of leaks, to verify the generalization ability of the video detection method for small leaks in buried gas pipelines proposed in this paper. The results of the multi-case leak detection experiments are shown in Figure 14.

Fig. 14, Fig. 14(a), and Fig. 14(b) show the detection results of the YOLOv5s model and the proposed buried gas pipeline tiny leak video detection model for the same frame image of the video, respectively. It can be observed in the



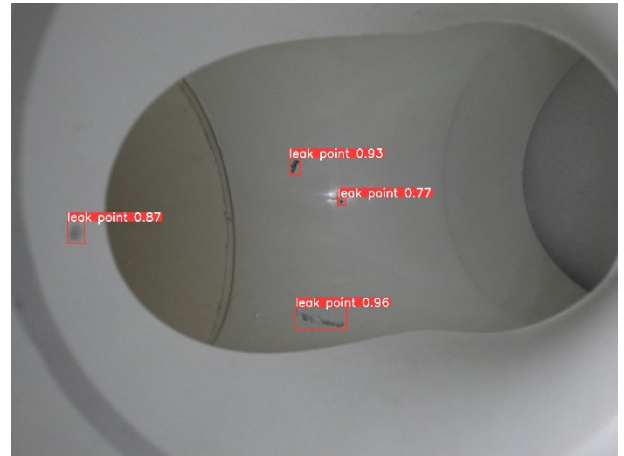
(a) detection results of YOLOv5s with holey structure and irregular shape leakage



(b) results of this paper's method for detecting leaks in porous structures and irregular shapes



(c) YOLOv5s test results at the tee



(d) test results of this paper's method at the tee



(e) test results of the YOLOv5s method at the joints of the two tubes



(f) test results of this paper's method at the joints of the two tubes

FIGURE 14. Multi-case leak detection results.

image that there are three leaks in the figure, one is a hole-like structure with tiny size, and the other two are irregularly shaped leaks with larger size than the hole-like tiny leaks.

From Fig. 14(a), it can be seen that the YOLOv5s model can detect the holey tiny leaks with a confidence level of 81%, and it can detect the irregularly shaped leaks above with a

confidence level of 73%, but it doesn't detect the irregularly shaped leaks at the bottom of the image, and leakage occurs, with a leakage rate of 33%. From Fig. 14(b), it can be seen that the buried gas pipeline tiny leakage video detection model proposed in this paper is also able to detect the hole-shaped tiny leakage and the irregular shape leakage above with a confidence level of 93%, which is 20% higher than that of the YOLOv5s model, and in the case of the irregular shape leakage below that isn't detected by the YOLOv5s model, the buried gas pipeline tiny leakage video detection model proposed in this paper is still able to detect the leakage. When the YOLOv5s model does not detect the irregularly shaped leak below, the video detection model proposed in this paper is still able to detect the leak with a confidence level of 95%.

Fig. 14, Fig. 14(c), and Fig. 14(d) show the detection results of the YOLOv5s model and the proposed buried gas pipeline tiny leakage video detection model for the same frame image of the video, respectively. It can be observed in the image that this image is located at the position of the pipe tee, and there are four leaks in the image, two of which are hole-like structures with tiny sizes, and the other two are irregularly shaped leaks with larger sizes. From Fig. 14(c), it can be seen that the YOLOv5s model can detect the pore-like tiny leaks on the right side with a confidence level of 69% and can detect the irregularly shaped leaks on the top side with a confidence level of 92%, but fails to detect the irregularly shaped leaks on the bottom side of the image and the tiny leaks on the left side of the pore-like structure, and two misses have occurred, with a miss detection rate of 50%. From Fig. 14(d), it can be seen that the video detection model of the buried gas pipeline tiny leakage proposed in this paper is also able to detect the hole-shaped tiny leakage on the right the irregular shape leakage on the top, and the confidence level is 77% and 93%, respectively, which is higher than that of the YOLOv5s model by 8% and 1%, respectively, and in the case of the YOLOv5s model, which does not detect the hole-shaped structure tiny leakage on the left and the irregular shape leakage on the bottom, it is not possible to detect the hole-shaped structure leakage on the left. When the YOLOv5s model does not detect the small leakage of the hole-like structure on the left side and the irregular shape leakage on the bottom side, the video detection model for the small leakage of the buried gas pipeline proposed in this paper is still able to detect the leakage there, and the confidence level is as high as 87% and 96%, respectively.

Fig. 14, Fig. 14(e), and Fig. 14(f) show the detection results of the YOLOv5s model and the proposed buried gas pipeline tiny leakage video detection model for the same frame image of the video, respectively. It can be observed in the image that this image is located at the position of the pipe elbow, and there are three leaks in the image, one of which is a hole-like structure with a small size, and the other two are irregularly shaped leaks with a large size. From Fig. 14(e), it can be seen that the YOLOv5s model can detect the irregular shape leak above with a confidence level of 40%, but it fails to detect the tiny leak of the pore-like structure in the image with the

irregular shape leak below it, and two leaks occur, with a leakage rate of 66.7%. From Figure 14(f), it can be seen that the buried gas pipeline micro-leakage video detection model proposed in this paper is also able to detect the irregularly shaped leaks above, and the confidence level is 96%, which is 56 percentage points higher than that of the YOLOv5s model, in the case that the YOLOv5s model does not detect the pore-like structure of the micro-leakage and irregularly shaped leaks below, the buried gas pipeline video detection model proposed in this paper is still able to detect the irregularly shaped leaks below. When the YOLOv5s model does not detect the tiny leak of the hole structure and the irregularly shaped leak below, the buried gas pipeline video detection model proposed in this paper is still able to detect the two leaks, and the confidence level is as high as 76% and 91% respectively.

From the above experiments, it can be learned that the method in this paper can detect leaks that are missed by the YOLOv5s model, and the method in this paper is also able to detect leaks that are detected by the YOLOv5s model, but the difference is that the confidence level of the method in this paper is higher than that of the YOLOv5s model. This paper proves that the method can detect leaks of different shapes, different sizes, and different pipeline paths, and has a strong generalization ability to realize the video detection of small leaks through leak detection experiments in many cases.

V. CONCLUSION

This paper proposes a video detection method for tiny leaks in buried gas pipelines in response to the difficult problem of tracking tiny leaks in buried gas pipelines. The method is based on the pipeline leakage dataset collected by the inspection robot in the buried gas pipeline, expanding the dataset, making the label corresponding to the dataset, and establishing the dataset. Introducing the BiFPN structure into the Neck layer in place of the original structure, enhancing the feature fusion ability of the model, and improving the precision of the model's leakage detection. Constructing the small-target detection layer based on the original structure of the Head layer, and adding a new small-target detection Head, to enhance the model's small leak detection ability. Send the data set into the proposed buried gas pipeline small leak video detection model, the model for parameter learning and network training. The collected buried gas pipeline small leak video into the trained model, the model's small leak video detection ability and small leak tracking ability to validate. Set up comparative experiments to prove that this paper's algorithms are better than the mainstream algorithms for target detection mainstream algorithms. Set up ablation experiments to prove that the higher evaluation index of this paper's method is due to the improvement of the YOLOv5s model. Set up a variety of leak detection experiments to prove that this paper's method can detect leaks of different shapes, leaks of different sizes, and leaks of different pipeline conditions, and it has a higher evaluation index and a better generalization ability. In summary, the video detection

method for small leaks in buried gas pipelines proposed in this paper has a better video detection effect, tracking ability, and generalization ability.

REFERENCES

- [1] A. Ebrahimi-Moghadam, M. Farzaneh-Gord, and M. Deymi-Dashtebayaz, "Correlations for estimating natural gas leakage from above-ground and buried urban distribution pipelines," *J. Natural Gas Sci. Eng.*, vol. 34, pp. 185–196, Aug. 2016.
- [2] K. Wang, X. Qian, and Z. Liu, "Experimental and numerical investigations on predictor equations for determining parameters of blasting-vibration on underground gas pipe networks," *Process Saf. Environ. Protection*, vol. 133, pp. 315–331, Jan. 2020.
- [3] N. Volgina, A. Shulgin, and S. Khlamkova, "Possibilities of diagnosis of stress corrosion cracking of main gas pipelines from the point of view of microbiology," *Mater. Today, Proc.*, vol. 38, pp. 1697–1700, Jan. 2021.
- [4] X. Li, Y. Zhang, R. Abbassi, M. Yang, R. Zhang, and G. Chen, "Dynamic probability assessment of urban natural gas pipeline accidents considering integrated external activities," *J. Loss Prevention Process Industries*, vol. 69, Mar. 2021, Art. no. 104388.
- [5] B. Thang and K. Jong-Myon, "Leak detection in a gas pipeline using spectral portrait of acoustic emission signals," *Measurement*, vol. 152, Feb. 2020, Art. no. 107403.
- [6] C. Capponi, S. Meniconi, P. J. Lee, B. Brunone, and M. Cifrodelli, "Time-domain analysis of laboratory experiments on the transient pressure damping in a leaky polymeric pipe," *Water Resour. Manage.*, vol. 34, no. 2, pp. 501–514, Jan. 2020.
- [7] X. Tian, W. Jiao, T. Liu, L. Ren, and B. Song, "Leakage detection of low-pressure gas distribution pipeline system based on linear fitting and extreme learning machine," *Int. J. Pressure Vessels Piping*, vol. 194, Dec. 2021, Art. no. 104553.
- [8] Y. Zhao, Z. Su, and H. Zhao, "Micro-leakage image recognition method for internal detection in small, buried gas pipelines," *Sensors*, vol. 23, no. 8, p. 3956, Apr. 2023.
- [9] H. Bai, X. Wang, Y. Guan, Q. Gao, and Z. Han, "Blood cell counting based on U-Net++ and YOLOv5," *Optoelectronics Lett.*, vol. 19, no. 6, pp. 370–376, Jun. 2023.
- [10] M. Tan, R. Pang, and Q. V. Le, "EfficientDet: Scalable and efficient object detection," in *Proc. IEEE/CVF Conf. Comput. Vis. Pattern Recognit. (CVPR)*, Jun. 2020, pp. 10778–10787.
- [11] K. Zhang, Y. Wu, J. Wang, Y. Wang, and Q. Wang, "Semantic context-aware network for multiscale object detection in remote sensing images," *IEEE Geosci. Remote Sens. Lett.*, vol. 19, pp. 1–5, 2022.
- [12] S. Chen, Y. Liao, F. Lin, and B. Huang, "An improved lightweight YOLOv5 algorithm for detecting strawberry diseases," *IEEE Access*, vol. 11, pp. 54080–54092, 2023.
- [13] K. Alex, S. Ilya, and H. Geoffrey, "ImageNet classification with deep convolutional neural networks," in *Proc. Adv. Neural Inf. Process. Systems.*, 2012, pp. 1097–1105.
- [14] M. Zeiler and R. Feergus, "Visualizing and understanding convolutional networks," in *Proc. Eur. Conf. Comput. Vis.*, 2014, pp. 818–833.
- [15] S. Kim, H. Kook, and J. Sun, "Parallel feature pyramid network for object detection," in *Proc. Eur. Conf. Comput. Vis. (ECCV)*, Munich, Germany, 2018, pp. 239–256.
- [16] S. Liu, L. Qi, H. Qin, J. Shi, and J. Jia, "Path aggregation network for instance segmentation," in *Proc. IEEE/CVF Conf. Comput. Vis. Pattern Recognit.*, Jun. 2018, pp. 8759–8768.
- [17] Y. Li, Y. Fan, S. Wang, J. Bai, and K. Li, "Application of YOLOv5 based on attention mechanism and receptive field in identifying defects of Thangka images," *IEEE Access*, vol. 10, pp. 81597–81611, 2022.
- [18] W. Liu, D. Anguelov, and D. Erhan, "SSD: Single shot MultiBox detector," in *Proc. 14th Eur. Conf. Comput. Vis. (ECCV)*, 2016, pp. 21–37.
- [19] K. He, X. Zhang, S. Ren, and J. Sun, "Spatial pyramid pooling in deep convolutional networks for visual recognition," *IEEE Trans. Pattern Anal. Mach. Intell.*, vol. 37, no. 9, pp. 1904–1916, Sep. 2015.
- [20] R. Girshick, "Fast R-CNN," in *Proc. IEEE Int. Conf. Comput. Vis. (ICCV)*, Dec. 2015, pp. 1440–1448.



YUXIN ZHAO received the bachelor's degree in automation from Beijing Information Science and Technology University, Beijing, China, in 2021, where he is currently pursuing the master's degree in navigation guidance and control. His current research interest includes target detection.



ZHONG SU (Member, IEEE) received the B.S. and M.S. degrees from the Beijing Institute of Technology, in 1983 and 1989, respectively, and the Ph.D. degree from the Beijing Institute of Vacuum Electronics Technology, in 1998. Currently, he is a Professor, the Ph.D. Supervisor, and the Director of the Beijing Key Laboratory of High Dynamic Navigation Technology and the Director of the Key Laboratory of Modern Measurement and Control Technology of the Ministry of Education of China, School of Automation, Beijing Information Science and Technology University, Beijing.



HAO ZHOU was born in Liaoning, in 1995. He is currently pursuing the master's degree with Beijing Information Science and Technology University. His current research interest includes robot motion control.



JIAZHEN LIN received the bachelor's degree in automation from Beijing Information Science and Technology University, Beijing, China, in 2021, where he is currently pursuing the master's degree in navigation guidance and control. His current research interests include navigation and localization.

...